The mystery of the Higgs particle/Le mystère de la particule de Higgs

Higgs searches at the LHC

Albert De Roeck [a,b,*], Giacomo Polesello [c]

[a] *CERN, CH-1211 Geneva, Switzerland*
[b] *University of Antwerp, Gratiekapelstraat 10-12, B-2000 Antwerpen, Belgium*
[c] *INFN, Sezione di Pavia, Via Bassi 6, 27100 Pavia, Italy*

Abstract

We review the prospects for searches of the Standard Model Higgs boson at the LHC, based on detailed studies performed by the ATLAS and CMS Collaborations. The search channels and strategies are described, resulting in the assessment of the discovery potential for the two experiments. We discuss the prospects for measurements in the Higgs sector. *To cite this article: A. De Roeck, G. Polesello, C. R. Physique 8 (2007).*
© 2007 Published by Elsevier Masson SAS on behalf of Académie des sciences.

Résumé

La recherche de la particule de Higgs au LHC. Nous passons en revue les perspectives de découverte au LHC du boson de Higgs du modèle standard, en nous basant sur les études détaillées des collaborations ATLAS et CMS. Les différents canaux de recherches ainsi que les stratégies adoptées sont décrits et permettent de quantifier le potentiel de découverte des deux expériences. Enfin, nous estimons les capacités de mesure dans l'ensemble du secteur de Higgs. *Pour citer cet article : A. De Roeck, G. Polesello, C. R. Physique 8 (2007).*
© 2007 Published by Elsevier Masson SAS on behalf of Académie des sciences.

Keywords: Higgs; LHC

Mots-clés : Particule de Higgs ; LHC

1. Introduction

The Higgs boson is the one piece of the Standard Model which has not yet found experimental confirmation. The search for the Higgs boson has become one of the highest priorities in today's experimental particle physics. After unsuccessful searches at LEP, and, to-date at the Tevatron, the relay passes to the LHC, the Large Hadron Collider, a proton–proton accelerator due to be commissioned in 2008. The LHC will be a unique tool for fundamental physics research and the highest energy accelerator in the world for many years following its completion. The LHC will provide two proton beams, circulating in opposite directions, at an energy of 7 TeV each (center-of-mass $\sqrt{s} = 14$ TeV). The nominal luminosity is expected to built up to 2×10^{33} cm^{-2} s^{-1} in the first years of operation, and will reach a maximum of 10^{34} cm^{-2} s^{-1} afterwards.

One of the main design requirements for the large general purpose experiments at the LHC has been the ability to detect the Higgs boson in the mass range between ~ 100 GeV$/c^2$ and 1 TeV$/c^2$, and the detector design has been optimised in order to achieve this goal.

A large amount of effort has been devoted by the two large Collaborations ATLAS and CMS to develop a search strategy optimising the potential of the two experiments for Higgs discovery. The results of this work have been documented in [1] and [2] for ATLAS, and more recently [3,4] for CMS. Earlier CMS results were summarised in [5]. At the time of writing of this report the ATLAS Collaboration is updating the studies on the Higgs potential, based on the understanding of the assembled detector and results will be available end of 2007. The existing information has already been summarised in an excellent review [6], which, however, was written when only partial results of the CMS studies were available. The main motivation for this review is therefore to update the results shown in [6] with the most recent results from the two experiments.

The characteristics of Higgs boson production and decay channels at the LHC are briefly described in Section 2. The main features of the ATLAS and CMS detectors will be described in Section 3. Section 4 is devoted to a review of the experimental strategy for Higgs discovery, and in Section 5 we will comment on the potential for the measurement of the properties of the Higgs boson at the LHC.

2. Higgs boson production and decay

We first summarise briefly the features of the Higgs production and decay necessary for our discussion. A more detailed discussion can be found in [7] and in the comprehensive review [8].

The Higgs production mechanisms are driven by the fact that the Higgs boson couples preferentially to the heavy particles, the W and Z bosons, the top quark and to a lesser extent the b quark. The main production processes at the LHC are:

– gluon fusion, $gg \to H$, at lowest order proceeding via a heavy quark loop;
– vector boson fusion (VBF), $qq \to qqH$;
– associated production of a Higgs boson with weak gauge bosons, $qq \to W/Z\, H$ (Higgs Strahlung);
– associated Higgs boson production with heavy quarks, $gg, qq \to ttH$, $gg, qq \to bbH$ (and $gb \to bH$).

The inclusive cross-section for all these processes have been calculated at NLO (except the single top associated process $qb \to qth$) and the processes $gg \to H + X$, $qq \to VH$ and $bb \to H + X$ have been calculated to NNLO in QCD ([9] and references therein). The QCD corrections to the transverse momentum and rapidity distributions are available for vector boson fusion and gluon–gluon fusion. A fully differential calculation at NNLO for the gluon fusion process has recently become available [10].

The LHC production cross-section calculated at NLO for the four processes is shown in the left panel of Fig. 1 (from [11]). Over the whole mass range considered, ranging to the lower limit from the LEP experiments to ~ 1 TeV$/c^2$, the dominant process is gluon–gluon fusion, with a cross-section ranging from ~ 50 pb in the vicinity of $m_H = 100$ GeV$/c^2$ to ~ 0.15 pb for 1 TeV$/c^2$. The second process in importance is vector boson fusion which has a significant cross-section over the full mass range. The cross-sections for production of the Higgs in association with W, Z and $t\bar{t}$ are smaller and these processes are relevant for the LHC searches only in vicinity of the low mass LEP limit.

The branching fractions of the Standard Model Higgs boson are shown in Fig. 1 (right panel) as a function of the Higgs boson mass. The calculations take into account both QCD and electroweak corrections. The branching ratio into WW and ZZ is dominant when kinematically accessible. The branching ratio into $t\bar{t}$ is $\sim 20\%$ when this decay is open. For masses well below the WW threshold region (< 140 GeV$/c^2$) the Higgs decays dominantly into two b quarks, the heaviest kinematically accessible fermion, with the decays $H \to \tau\tau$ and $H \to gg$ both at the level of $\sim 8\%$ for Higgs masses between 100 and 130 GeV$/c^2$. The decay into two photons proceeds via fermion and W loops and has a branching fraction of up to 2×10^{-3} for low masses. This decay, as we will see, plays a crucial role in the experimental searches.

The total Higgs decay width is negligible compared to the experimental resolution for low masses, and only becomes relevant above the ZZ threshold. Above ~ 1 TeV$/c^2$ the decay width becomes comparable to the mass of the Higgs particle.
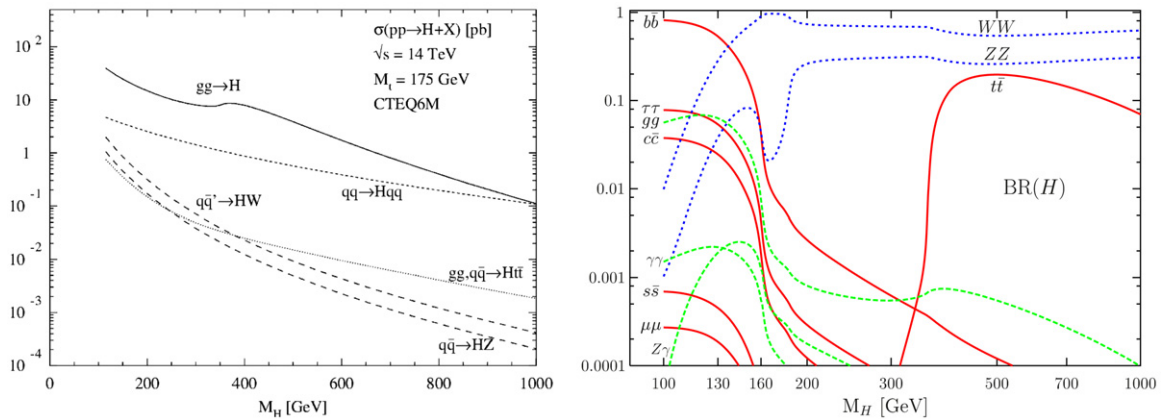
Fig. 1. Left: The SM Higgs production cross-section at the LHC as a function of the Higgs mass for the main processes. Right: The SM Higgs bosons decay branching fractions as a function of the Higgs mass (from Ref. [11]).

Table 1
Production and decay modes for Higgs particles with mass less than 200 GeV/c^2 that have been studied by the LHC experiments

Decay	Production			
	Inclusive	VBF	WH/ZH	ttH
$H \to \gamma\gamma$	yes	yes	yes	yes
$H \to bb$			yes	yes
$H \to \tau\tau$		yes		
$H \to WW^{(*)}$	yes	yes	yes	
$H \to ZZ, Z \to ll$	yes			
$H \to Z\gamma, Z \to ll$	low σ			

Table 1 shows an overview of the production and decay combinations that are accessible at the LHC. These will be discussed in the following.

3. The LHC experiments

Two large general purpose experiments ATLAS (A Toroidal LHC Apparatus) and CMS (Compact Muon Solenoid) are in the final assembly phase, and will be ready to take data at the LHC startup currently foreseen for summer 2008.

A schematic view of the two detectors is shown in Figs. 2 and 3.

The LHC will open up the exploration of the TeV energy range. In order to be able to fully exploit the discovery opportunities offered by the LHC, the two detectors are conceived as multi-purpose, and will provide efficient and precise measurements of electrons, muons, taus, neutrinos, photons, light flavour jets, *b*-jets and the missing transverse momentum.

Detailed descriptions of the two detectors are available in the Technical Proposals and Technical Design Reports [12,13]; only a brief summary of the main design choices is given in the following. The main features of the two experiments are summarised in Table 2.

CMS is centered around one magnet, a big solenoid, which contains the inner detector and the calorimeters and provides a magnetic field of 4 T in the inner detector volume. ATLAS has four magnets: a solenoid sitting in front of the electromagnetic calorimeter and producing a field of 2 T in the inner cavity, and external barrel and end-cap air-core toroids. The general structure of the two detectors is determined by this basic design choice.

Both detectors reconstruct the tracks from the interaction vertex using inner detectors built of layers of silicon pixel and silicon strip detectors immersed in the solenoidal magnetic field. These detectors provide a high precision measurement of the vertex position and of the track momenta. While the CMS tracking detector is all silicon, the ATLAS inner detector in addition contains a Transition Radiation Detector (TRT) at larger radii. Excellent momentum
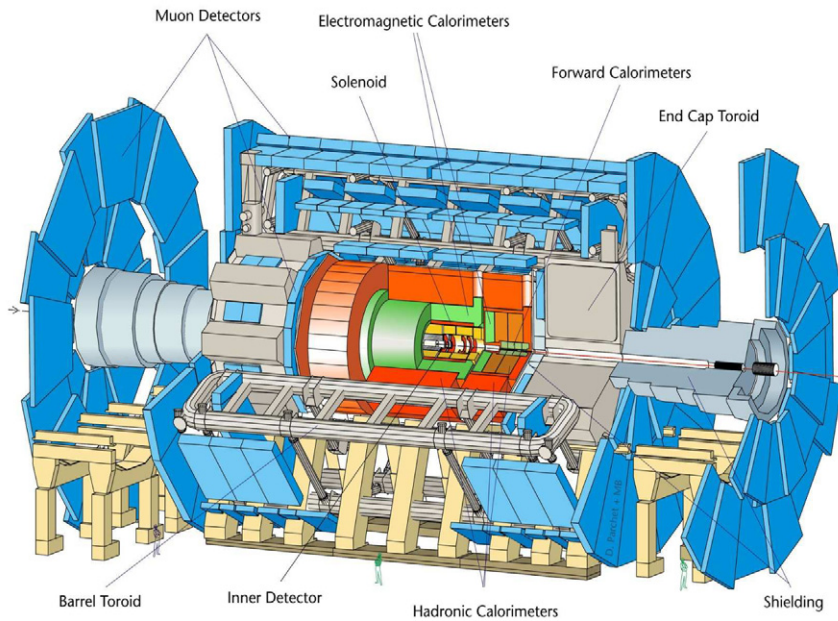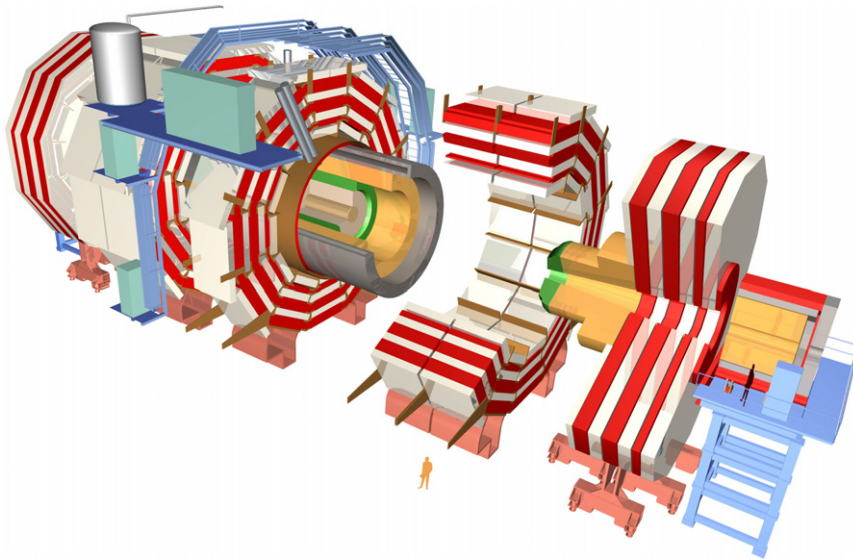
Fig. 2. Schematic view of the ATLAS detector.

Fig. 3. Schematic view of the CMS detector.

resolution is expected for both experiments as shown in Table 2 (see [14]). Due to the lower magnetic field the expected momentum resolution in ATLAS is a factor of about two worse than that of CMS. However, the Transition Radiation Detector provides electron/pion separation capabilities. Thanks to silicon strip and pixel detectors, both experiments will be able to perform b quark tagging using impact parameter measurements and the reconstruction of secondary vertices. As we will see below, this capability is essential for many of the Higgs channels discussed in the following.

The CMS electromagnetic calorimeter is a high-resolution lead tungstate ($PbWO_4$) crystal detector. The ATLAS calorimeter is a lead-liquid argon sampling calorimeter, therefore with a worse intrinsic energy resolution. However, thanks to a very fine lateral and good longitudinal segmentation, the ATLAS calorimeter potentially has more robust

Table 2
Main features of the ATLAS and CMS detectors

	ATLAS	CMS
Magnet(s)	Air-core toroids + solenoid in inner cavity	Solenoid
	Calorimeters in field-free region	Calorimeters inside field
	4 magnets	1 magnet
Inner detector	Si pixels and strips	Si pixels and strips
	TRT → particle identification	No particle identification
	B = 2 T	B = 4 T
	$\sigma/p_T \sim 3.4 \times 10^{-4} p_T\,(\mathrm{GeV}) \oplus 0.01$	$\sigma/p_T \sim 1.5 \times 10^{-4} p_T\,(\mathrm{GeV}) \oplus 0.008$
EM calorimeter	Lead-liquid argon	$PbWO_4$ crystals
	$\sigma/E \sim 10\%/\sqrt{E\,(\mathrm{GeV})}$	$\sigma/E \sim 3 - 5\%/\sqrt{E\,(\mathrm{GeV})}$
	Longitudinal segmentation	No longitudinal segmentation
HAD calorimeter	Fe-scintillator + Cu-liquid argon	Brass-scintillator
	$\geqslant 10\,\lambda$	$\geqslant 7.2\,\lambda$ + tail catcher
	$\sigma/E \sim 50\%/\sqrt{E\,(\mathrm{GeV})} \oplus 0.03$	$\sigma/E \sim 100\%/\sqrt{E\,(\mathrm{GeV})} \oplus 0.05$
Muon spectrometer	Chambers in air	Chambers in solenoid return yoke (Fe)
	$\sigma/p_T \sim 7\%$ at 1 TeV	$\sigma/p_T \sim 5\%$ at 1 TeV
	Spectrometer alone	Combining spectrometer and inner detector

particle identification capabilities. The design of the electromagnetic calorimeters has been mainly driven by the $H \to \gamma\gamma$ discovery channel, which requires excellent energy and angular resolution as well as a high rejection power on jets faking photons.

In both experiments the hadronic calorimeters are sampling detectors with scintillator or liquid-argon as active medium. The ATLAS hadronic calorimeter offers a better energy resolution because it is thicker (the CMS hadronic calorimeter is constrained in space as dictated by the external solenoid dimensions) and has a finer sampling. CMS will be using particle flow techniques to improve the resolution of the calorimeter response. For both experiments the calorimetric coverage is extended down to a rapidity of $|\eta| < 4.9$ in order to ensure hermetic coverage for the measurement of missing transverse momentum, and to allow the detection of forward jets, which constitute an important signature for many physics processes, including the Higgs production in vector boson fusion.

Finally, the external Muon spectrometer of CMS consists of chamber stations embedded into the saturated iron of the solenoid return yoke, thus achieving a design where a single magnet provides the necessary bending power for precise tracking in the inner detector and in the muon spectrometer. ATLAS has a spectrometer in air, where multiple scattering is minimised, and therefore offers the possibility of good standalone (i.e. without the inner detector contribution) muon momentum measurement with three stations of high-precision tracking chambers at the inner and outer radius and in the middle of the air-core toroid. The expected momentum resolution is better than 10% for muons of $p_T = 1$ TeV/c in both experiments.

4. Perspectives for Higgs discovery

The main challenge for searches of new physics at hadron colliders is the reduction of the overwhelming background from QCD jets which is produced with a cross-section which is many orders of magnitude larger than the signal. For this reason the basic strategy is based on the identification of signatures involving leptons or photons in the final state. For $M_H > 160$ GeV/c^2, the Higgs decays mainly into $WW^{(*)}$ and $ZZ^{(*)}$, which in turn decay with a significant branching fraction into leptons. The 'golden' channel for Higgs discovery in this mass range is therefore $H \to ZZ^{(*)} \to 4\ell$, supplemented by $H \to ZZ^{(*)} \to \ell\ell\nu\nu$, $H \to ZZ^{(*)} \to \ell\ell jj$ and $H \to WW \to \ell\nu jj$ for $M_H > 600$ GeV/c^2, where the production cross-section becomes smaller. For M_H below 140 GeV/c^2, the main inclusive decay mode $H \to bb$ is hopeless, as is $H \to \tau\tau$. Thus the most promising inclusive channel turns out to be the rare decay $H \to \gamma\gamma$.

Another possibility is the associated production of the Higgs with W, Z and t. In this case the triggering lepton is provided by the accompanying particle, and the lower production cross-section is compensated by the fact that the Higgs can be searched for in its dominant bb decay mode.

Finally, a special class of processes is vector boson fusion, whose importance for the Higgs search strategy was recognised only relatively recently. In this case the Higgs is produced in association with jets with a very specific

topology. This provides an additional signature, which allows the selection of the Higgs decays into experimentally more difficult channels such as $H \to \tau\tau$.

It is convenient to review separately the different search strategies, as they present different experimental challenges, ranging from very severe requirements on photon/lepton identification measurement for inclusive searches to the handling of complex event topologies in the associate searches. We will show at the end the combined results to assess the complete discovery potential of the experiments.

A general issue in showing the ATLAS and CMS alongside is the fact that signal and background rates are calculated by ATLAS at leading order, whereas CMS takes into account the NLO QCD corrections for both signal and background through the use of K-factors and NLO event generators. The ATLAS approach was motivated by the fact that the Monte Carlo generators for the signal and background estimates available at the time when the ATLAS results where produced, such as PYTHIA, only implement LO calculations, and the estimate of the effect of higher order corrections (when available) through a straight K-factor can be misleading, as the experimental selection cuts can select phase space regions where the total effect of radiative correction is different from the one obtained rescaling the inclusive cross-section. However, in recent years a significant progress has been made both in the evaluation of NLO cross-sections for most of the relevant background process, and in the implementation of the processes in NLO Monte Carlo generators, which allows a more solid evaluation of the signal significance based on the most advanced theoretical calculations. CMS has used these calculations and tools in their recent studies. The forthcoming ATLAS updated results will also take advantage of the new tools.

4.1. Inclusive searches

In this class of searches, where the experiments only focus on the decay products of the Higgs, we will address the main channels $H \to \gamma\gamma$, $H \to ZZ^{(*)}$, $H \to WW^{(*)}$.

4.1.1. $H \to \gamma\gamma$ decay

The $H \to \gamma\gamma$ decay has been recognised from the very early studies of LHC physics as the most promising inclusive signature for Higgs masses ranging from the LEP limit to approximately 135 GeV/c^2.

The signal would appear as a narrow peak in the invariant mass of a photon pair over a continuum background. This background has two components: the irreducible QCD $\gamma\gamma$ production and a reducible component from γ-jet and jet-jet production where one or both of the hadronic jets are misidentified as a photon. Even after the reducible background is reduced well below the irreducible $\gamma\gamma$ background, this channel is quite challenging due to the low branching fraction for photons and to the high QCD cross-section. For an integrated luminosity of 20 fb^{-1} and for a Higgs mass of 120 GeV/c^2 one expects approximately 300–400 signal events for a background of 7000–8000 events. In order to optimise the signal to background ratio the signal peak has to be as narrow as possible. Two components affect the width of the peak: the energy resolution for the photons and the resolution on the direction of the two photons. The CMS calorimeter has a superior energy resolution, but no possibility to measure the position of the interaction vertex from the standalone calorimetric measurements. They rely therefore on the measurement of the vertex from tracks from the hadronic activity accompanying the Higgs production. The ATLAS electromagnetic calorimeter has a lower resolution, but a very high longitudinal and lateral segmentation, allowing the reconstruction of the interaction vertex from the calorimeter alone. This feature is particularly useful at high luminosity where the presence of many vertices may make the identification of the Higgs interaction vertex complex. Through a realistic detector simulation it has been shown that the reducible background can be brought to a level of $\sim$20% of the irreducible one, using selection criteria on the photon isolation and on the shower shape in the calorimeter. The two photons are requested to be inside a pseudorapidity range of $|\eta| < 2.4(2.5)$, and the total acceptance after the kinematic selection and identification cuts ranges between 20 and 30% in the mass range 110–150 GeV/c^2. The distribution of the photon-photon invariant mass over the background for four Higgs masses is shown in Fig. 4 for the CMS experiment.

The background evaluation is performed through the study of the sidebands of the peak, and is therefore not affected by uncertainties on the theoretical cross-section. The main systematic uncertainty is thus from the choice of the functional shape for the background and contributes with an error of 0.5%. With a simple cut-based analysis, the CMS experiment quotes a 5σ discovery potential for Higgs masses between 115 and 145 GeV/c^2 for an integrated luminosity of 30 fb^{-1}. The results of ATLAS are similar, once the difference due to LO/NLO cross-sections choice and difference in the analysis is accounted for.
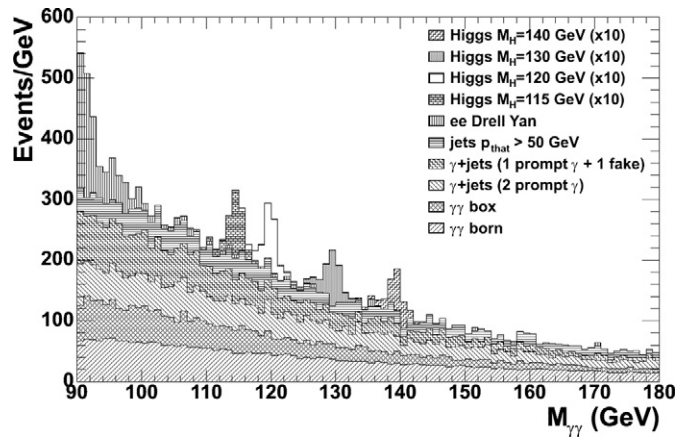
Fig. 4. Diphoton invariant mass spectrum after the selection for a cut-based analysis. Events are normalised to an integrated luminosity of 1 fb^{-1} and the Higgs signal, shown for different masses, is scaled by a factor 10 (from Ref. [4]).

A more sophisticated analysis based on neural networks to exploit the kinematic differences in signal and background was recently performed by the CMS Collaboration. An improvement in significance is observed which, under the condition that an adequate understanding of the kinematic distributions for background is achieved, would give a strong hint for Higgs discovery already in the first year of good data taking at the nominal start-up luminosity. Using this technique the amount of data needed to discover a Higgs particle with mass with 130 GeV/c^2 or less is 8–10 fb^{-1}.

4.1.2. $H \rightarrow ZZ^{(*)}$ decay

One of the most promising roads for the Higgs discovery is via the decay into charged leptons, $H \rightarrow ZZ^{(*)} \rightarrow l^+l^-l^+l^-$ (in short $H \rightarrow 4l$) which offers a possibly significant and very clean and simple multi-lepton final state signature. Ultimately, the channel can provide a precision determination of the Higgs boson mass and production cross-section. The anti-correlation of the Z spin projections in the $H \rightarrow ZZ$ decay and the polarisation of each Z boson can be used to constrain, and eventually determine, the spin and CP quantum numbers of the Higgs resonance for Higgs masses larger than 200 GeV/c^2. Furthermore, the $ZZ^{(*)}$ and $WW^{(*)}$ decay modes are related via $SU(2)$ and the combination of channels could allow for cancellation of some systematic uncertainties in a determination of the Higgs coupling. The $H \rightarrow ZZ \rightarrow ll$ jet jet and $H \rightarrow ZZ \rightarrow ll\nu\nu$ channels are used for heavy Higgses. The main backgrounds for this channel are $ZZ^{(*)}$, $Z\gamma^{(*)}$, and the reducible backgrounds from $t\bar{t}$ and $Zb\bar{b}$ associated production. It has been shown by both experiments that the reducible backgrounds can be reduced below the level of the irreducible ones through a combination of cuts on lepton isolation and impact parameters.

The main result of the previous LO studies is that the Higgs can be observed in this channel with a luminosity of 30 fb^{-1} in the mass range $130 < m_H < 700$ GeV/c^2, except for a narrow region near 170 GeV/c^2, corresponding to the opening up of the on-shell WW decay.

CMS has recently revisited this channel in detail in its physics TDR. Backgrounds from $ZZ^{(*)}$, $t\bar{t}$ and $Zb\bar{b}$ associated production are taken into account. The decay channels into 4 electrons, 4 muons and 2 electrons + 2 muons have been studied, all taking into account the corresponding trigger tresholds for multi-lepton channels. The Monte Carlo samples were normalised to represent the NLO cross-sections, including mass dependent K-factors. A full treatment of the most important theoretical and instrumental systematic errors and their effect on the evaluation of significance of the Higgs boson observation as well as measuring its parameters were included.

For the $H \rightarrow eeee$ channel several quality classes of electrons have been defined, based on their detailed experimental characterisation, resulting from possible showering and interaction in the material before the electromagnetic calorimeter. The expected number of signal and background events are evaluated with a sliding window whose central position m_{4e} varies between 100 and 320 GeV/c^2. The size of the optimal window increases progressively from 6 GeV/c^2 at $m_{4e} = 115$ GeV/c^2 to 24 GeV/c^2 at $m_{4e} = 300$ GeV/c^2. The significance for this channel is shown in Fig. 5(left).

The signal over background for the $H \rightarrow \mu\mu\mu\mu$ process is shown in Fig. 5(right) for several Higgs mass values. Both a search using $m_{4\mu}$ dependent and independent cuts have been used. The Higgs boson discovery potential
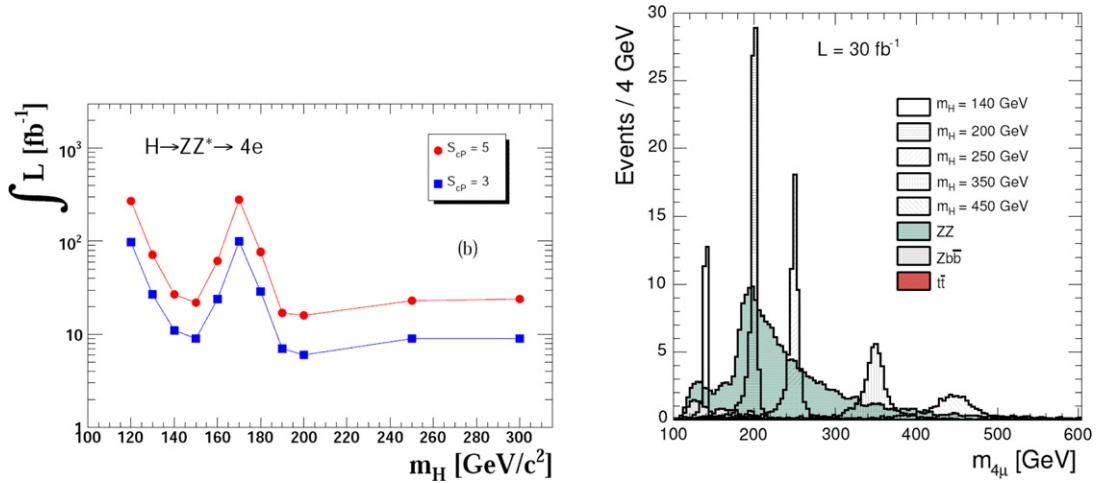
Fig. 5. (Left) luminosity needed for a 3σ observation and 5σ discovery of the process $H \to eeee$, with the systematics included using $ZZ^{(*)}$ normalisation to the Z cross-section. (Right) $H \to \mu\mu\mu\mu$ reconstructed four-muon invariant mass distribution, for an integrated luminosity of 30 fb^{-1}, for background (shaded histograms) and several Higgs signals (hatched), after the selection criteria are applied (from Ref. [4]).

was explored for different analysis variations, including the use of $m_{4\mu}$-dependent and flat cuts, log-likelihood ratio based on the full $m_{4\mu}$ spectrum and a straightforward counting experiment approach. A discovery at the level of 5σ significance could be already possible with ~ 10 fb^{-1} for m_H in the range 140 GeV/c^2–150 GeV/c^2 and 190 GeV/c^2–400 GeV/c^2.

Finally, also the mixed lepton flavor channel $Z \to ee\mu\mu$ has been studied. Fig. 6 shows the number of expected events for signal and background for an integrated luminosity corresponding to a discovery significance of 5σ, for Higgs boson masses of 140 and 200 GeV/c^2. Including this channel enhances the statistical power for a discovery substantially.

The combined discovery reach of the $H \to ZZ$ channel is shown in Fig. 14.

4.1.3. $H \to WW^{(*)}$ decay

The Higgs decay into two Ws and subsequently decay into two leptons ($H \to WW \to \ell\nu\ell\nu$) is the most promising discovery channel for Higgs boson masses between $2m_W$ and $2m_Z$ [15]. In this mass range, the Higgs to WW branching ratio is close to one, leading to a large number of produced events. The signal signature is characterised by two leptons in the final state with opposite charge, missing energy and no jet. However, since no narrow mass peak can be reconstructed, good understanding of the background together with a high signal to background ratio is needed. The selection is therefore typically optimised for a Higgs mass of 165–170 GeV/c^2, and studied for the muon and electron final states. The most important backgrounds, which give a similar signature as the signal are the continuum WW production and $t\bar{t}$ and tWb production. To reduce these backgrounds, one has to require a small opening angle between the leptons in the transverse plane and apply a jet veto. Fig. 7(left) shows the distribution of the angle between the leptons in the transverse plane for the signal and the different background for a luminosity of 10 fb^{-1}.

It turns out that this channel has the highest sensitivity, if the Higgs is close in mass to the WW threshold. Combined with the muon channel a discovery is possible with 1 fb^{-1} if the mass of the Higgs is indeed around 160 GeV/c^2. The signal can be detected with a 5σ significance for masses between 150 and 190 GeV/c^2 and an integrated luminosity of 10 fb^{-1}, provided that a systematic control of the backgrounds to a 5% level is achieved.

A dedicated optimisation for the $e^+e^-\nu\nu$ final state in the mass range of $130 \leqslant M_H \leqslant 150$ GeV/c^2 has been performed as well. An example of the signal for 10 fb^{-1} is shown in Fig. 7(right). Including backgrounds uncertainties and systematics a significance of about 4σ can be obtained for Higgs masses in the range of 140–150 GeV/c^2.

This decay channel, in the mode $H \to WW \to \ell\nu jj$ can also be used to extend the mass reach of the LHC experiments up to 1 TeV, profiting from the large gain in branching fraction with respect to the ZZ channel.
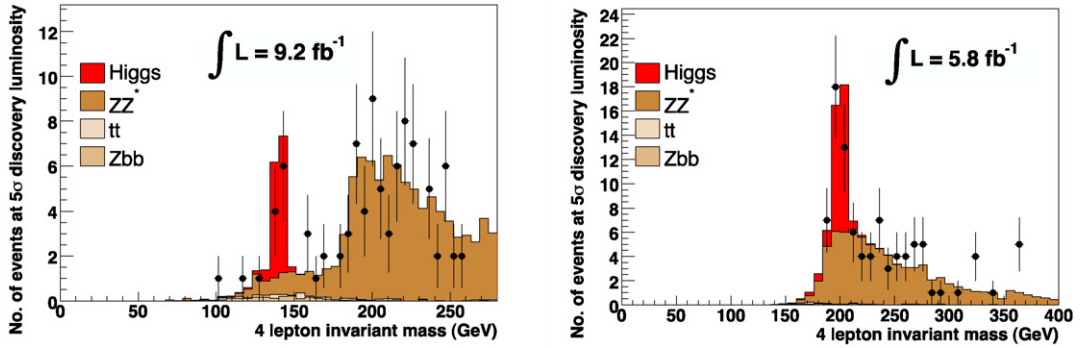
Fig. 6. Number of expected events for signal and background for an integrated luminosity corresponding to a discovery significance of 5σ, for Higgs boson masses of 140 GeV/c^2 (left) and 200 GeV/c^2 (right). The results of a simulated experiment are also shown to illustrate the statistical power of the analysis and the determination of the background normalisation from data (from Ref. [4]).
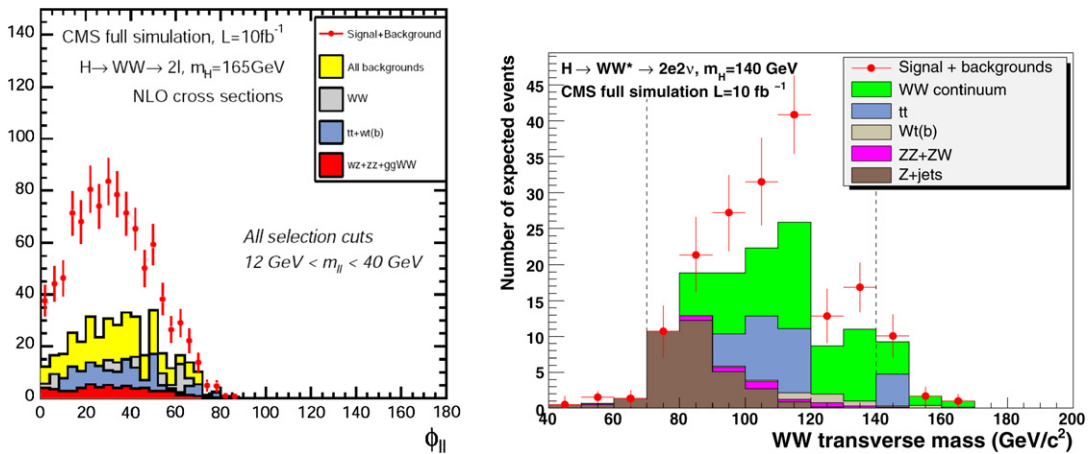

Fig. 7. (Left) The angle between the leptons in the transverse plane for the signal and the different backgrounds for a luminosity of 10 fb^{-1}; (Right) the reconstructed WW transverse mass for a 140 GeV/c^2 Higgs signal selection with 10 fb^{-1} (from Ref. [4]).

4.2. Associated production

To improve signal over background ratio in Higgs searches, it can be advantageous to turn to the associated production channels: a Higgs produced in association with a vector boson or a heavy flavour quark, e.g. a top quark.

The associated production with W, Z bosons is a well known search channel at the Tevatron, and uses the leptonic decay channels of the Z and W. These leptons, which have in general a high p_T, allow to suppress efficiently QCD backgrounds. The penalty is a considerably lower cross-section for the production, as shown in Fig. 1.

At the LHC the searches WH, with $H \to \gamma\gamma$ and bb, have been studied. Given that the direct search for inclusive $H \to bb$ is swamped by background, this is a possible channel to access the Higgs to b-quark coupling. The analyses so far show that even with 30 fb^{-1} the statistical sensitivity of this channel is at best about 2σ [1,5] and thus it will remain a difficult channel which needs very large statistics before any meaningful information can be extracted from it.

Possible other associated channels $ZH \to llbb$, $ZH \to \nu\nu bb$ and $bbH \to bbbb$ have been suggested for observing $H \to bb$ but these have not yet been considered for a low mass SM Higgs boson due to the challenging trigger and background conditions.

The channel WH, ZH with $H \to \gamma\gamma$ has been studied with full simulation both in the ATLAS and in the CMS detector. A statistical significance of about 4σ can be reached with 100 fb^{-1} for a Higgs boson with mass of 120 GeV/c^2.

Associated production of the Higgs boson with top quarks is another method to try to suppress much of the QCD background. In particular earlier studies, based on fast simulation, both from ATLAS and CMS had the promise that

the channel $ttH \rightarrow ttbb$ could be accessible and hence provide information on the Higgs to bb coupling. Recently CMS has made a detailed study based on full simulation, more realistic b-tagging and backgrounds calculated with ALPGEN [16]. Important backgrounds to this process are top quark pair production plus one or more jets, both for light and b-quark jets. The result shows that the Higgs boson reconstruction is significantly less promising than that derived from earlier studies, and instead of bump hunting, the analysis becomes a counting experiment. It is then important that the background is well controlled from real data and several techniques to use the data for background determination were designed and used to constrain the background uncertainties for this measurement. All final states such as $bbbbqq\mu\nu$, $bbbbqqe\nu$, $bbbbl\nu l\nu$, $bbbbqqqq$ have been used and combined. Generally 3 b-jets were required to be tagged. Systematic errors have been estimated and – apart from the background uncertainty – the dominant ones have been found to be the jet energy scale and resolution, and the b-tagging efficiencies. The result shows that for a Higgs with mass in the range of 115–130 GeV/c^2 even with 60 fb^{-1} of integrated luminosity the significance is marginal and below 2σ if the uncertainty on the background will be a few % or more. Hence, contrary to the earlier fast simulation results, it looks like that this channel will be very difficult to access at the LHC. Some improvements are still under study and notably a particle flow method to reconstruct the final state of the Higgs could help to resurrect the measurability of this channel. ATLAS is also redoing the study with full simulation. There are hopes that the outcome will be more optimistic due to the better hadronic calorimetry of ATLAS, allowing a better reconstruction of the Higgs decay into b-quarks.

Also the associated channel ttH, $H \rightarrow \gamma\gamma$ has been studied, taking into account all backgrounds as for the inclusive channel, some of which are irreducible as discussed before. The signal to background ratio that can be achieved after suitable cuts is 4:1. A signal observability in excess of 3σ can be obtained for Higgs masses up to 130 GeV/c^2, including systematic errors, for an integrated luminosity of 100 fb^{-1}.

Finally the channel WH, $H \rightarrow WW^{(*)} \rightarrow 2l2\nu$ has been studied. For the Higgs mass range 120–190 GeV/c^2 the cross-section exceeds 300 fb, and final states with 3 leptons and missing transverse momentum were investigated. When a jet veto is applied then the most important backgrounds left are WWW and ZZ production. In total, an order of 50 to 100 fb^{-1} of integrated luminosity is needed for a 5σ discovery in this channel. Hence the inclusive $H \rightarrow WW$ production should be observable much before this channel. This Higgs decay channel has also been studied in association with tt in [17] and preliminary results show a signal to background ratio of 1:1 and a statistical significance of about 3σ for an integrated luminosity of 30 fb^{-1}. The challenge to observe this process will be to control the background, which presently is subject to large uncertainties and requires more detailed studies.

In all, the associated production processes are expected to contribute to the Higgs searches and analyses for luminosities larger than 30 fb^{-1}.

4.3. Vector boson fusion

The second largest contribution to Higgs production at the LHC is vector boson fusion. In this processes two quarks in the initial-state protons radiate two W or Z bosons, which in turn interact to produce a Higgs boson. This process accounts for $\sim$20% of the Higgs production cross-section below the ZZ threshold, increasing with Higgs mass. The Higgs boson is accompanied by two jets in the forward region of the detector from the hadronisation of the initial quarks emitting the vector bosons. Moreover, due to the lack of colour exchange between the quarks, central jet activity is suppressed with respect to most background processes. It is therefore possible to enhance the signal-to-background ratio by tagging the two jets in the forward region of the detector and by applying a veto on central jets or any other hadronic activity. Phenomenological studies have pointed out that this signature, originally studied for high-mass Higgs can provide a significant enhancement of the Higgs discovery potential in the intermediate mass region. Thanks to the additional constraints to the initial state, Higgs decays such as $H \rightarrow WW^{(*)}$ and $H \rightarrow \tau^+\tau^-$ can be studied. Besides enhancing the sensitivity these modes provide the possibility of measurement of otherwise unaccessible decays of the Higgs boson.

The tagging of jets in the high rapidity region has been studied with detailed simulation both in ATLAS and in CMS. The tag jets are identified in the analysis as the two jets with highest pseudorapidity. With this algorithm the tag jets are efficiently identified, as shown in Fig. 8 where the rapidity distribution (left) and the rapidity separation (right) of the tag jets from the parton level information are shown as a full line, and where the points with error bar show the distribution for the jets reconstructed with the above described algorithm. The distribution for $t\bar{t}$ events is shown as a dashed line, demonstrating the high rejection power of jet tagging. An additional issue is the efficiency
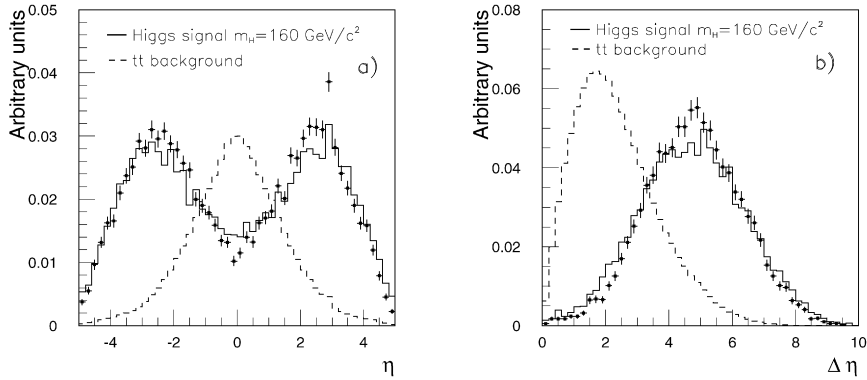
Fig. 8. (Left) Pseudorapidity distribution of the tag jets in signal events with $m_H = 160$ GeV/c^2 and for $t\bar{t}$ background events. (Right) Separation $\Delta\eta$ between the tag jets for the same types of events. The full histograms show the distributions at parton level, the dots represent the distributions at reconstruction level, after the tagging algorithm has been applied. The corresponding distributions for jets identified as tag jets in $t\bar{t}$ events are superimposed as dashed histograms. All distributions are normalised to unity (from Ref. [2]).

for the reconstruction of jets at high rapidity in the presence of pile-up. From a detailed study in ATLAS it has been found that a reasonable reconstruction efficiency for jets with $p_T > 20$ GeV/c is achieved up to rapidity 4.9.

The pile-up (and also the underlying event) may also affect the jet veto cut, by creating fake central jets in the Higgs events through fluctuations in the minimum bias events, thus reducing the selection efficiency. From a detailed ATLAS study it has been found that through appropriate handling of the calorimeter signal, the fraction of events with a fake jet can be kept at the few percent level at nominal start-up luminosity (10^{33} cm^{-2} s^{-1}) for jets with $p_T > 20$ GeV/c.

A typical jet selection for the following analyses is therefore the request of two jets with high rapidity separation $|\eta_{j1} - \eta_{j2}| > 3.8$, and the veto of any other jet with $p_T > 20$ GeV/c within $|\eta| < 3.2$.

4.3.1. The $qqH \rightarrow qqWW^{(*)}$ channel

This channel has been studied in two final-state signatures: the fully leptonic one $H \rightarrow WW^{(*)} \rightarrow \ell\nu\ell\nu$, and the semileptonic one $H \rightarrow WW^{(*)} \rightarrow \ell\nu jj$ where one of the two W bosons is searched for in its hadronic decay.

The dominant background is $t\bar{t}$. Other relevant backgrounds considered in the experimental analyses are QCD WW + jets production, electroweak WW + jets production, QCD γ/Z + jets production, electroweak $\tau\tau$ + jets production and ZZ production. The electroweak backgrounds have low cross-section, but high acceptance because their color flow is similar to the one for the signal. The signature for the fully leptonic channel are two leptons and E_T^{miss}. The main handle for the rejection of backgrounds is the kinematics of the two leptons. Since the W^+ and the W^- are produced with opposite spins, the lepton and the antilepton are emitted preferentially in the same direction, contrarily to the WW and $t\bar{t}$ backgrounds where they are emitted approximately back to back. Cuts are therefore applied on the azimuthal and polar angular separation of the two leptons. Moreover, in this kinematic situation, the lepton–lepton invariant mass is bound to be smaller than $M_H/2$. The transverse invariant mass of the two leptons with E_T^{miss} exhibits a Jacobian peak at the Higgs mass, whereas the Drell–Yan background peaks around zero. After application of the jet and lepton cuts, and veto of b and τ jets, for $m_H = 160$ GeV/c^2 the accepted signal cross-section is ~ 4.6 pb for a background cross-section of ~ 1.6 pb. The Higgs mass cannot be directly reconstructed in this channel, because of the two neutrinos. The W are, however, produced approximately at rest in the Higgs rest frame, resulting in $m_{\ell\ell} \sim m_{\nu\nu}$, and a transverse mass variable m_T for the dilepton system can be calculated which is a good approximation of the Higgs mass. The distribution for this variable for the signal after the jet cuts is shown in Fig. 9 superimposed to the same distribution for the signal. A clear kinematic evidence for the signal can be seen in this distribution, as well in the distribution of the azimuthal separation of the two leptons. This channel has an excellent discovery potential. Already with 10 fb^{-1} this channel would allow a 5σ discovery for $M_H > 130$ GeV/c^2.

The semileptonic channel $H \rightarrow WW^{(*)} \rightarrow \ell\nu jj$ has a larger branching fraction, but also much larger background, since the request of a single lepton in the final state makes this signature vulnerable to the large W + jets background. A very tight jet veto is required in order to obtain a significant signal. In these conditions, from a CMS optimised analysis, a signal can be observed with 5σ significance for M_H between 140 and 200 GeV/c^2 for 30 fb^{-1}. The large
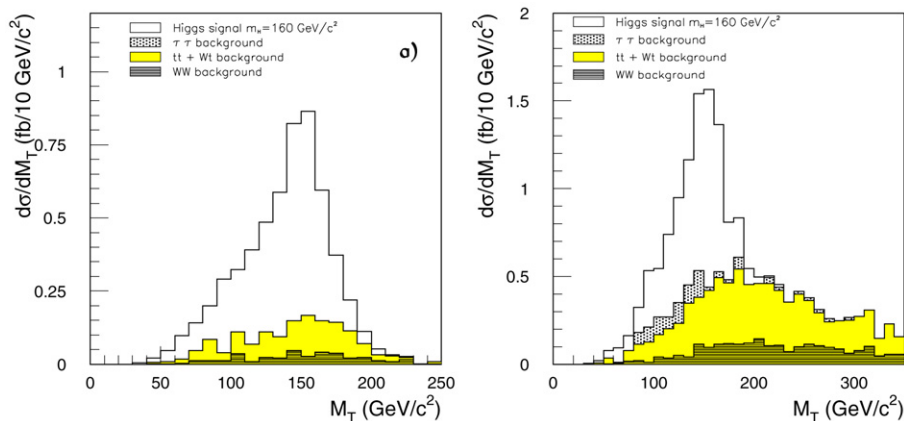
Fig. 9. (Left) Distribution of the transverse mass M_T for a Higgs boson with a mass of 160 GeV/c^2 and the backgrounds in the $e\mu$-channel after all cuts. (Right) The same, after relaxing kinematic cuts on the reconstructed leptons. The accepted cross-sections $d\sigma/dM_T$ (in fb/10 GeV/c^2) including all efficiency and acceptance factors are shown in both cases (from Ref. [2]).

$W +$ jets background and the very tight cuts required to extract this signal may induce however large systematic uncertainties on the background estimate.

4.3.2. The $qqH \rightarrow qq\tau^+\tau^-$ channel

The vector boson fusion production of a Higgs boson followed by decay to two τs provides a viable signal for M_H between 100 and 140 GeV/c^2. The search potential has been studied for $H \rightarrow \tau\tau$ decays using the double leptonic decay mode $qqH \rightarrow qq\tau\tau \rightarrow qq\ell\nu\bar{\nu}\ell\bar{\nu}\nu$ and the lepton–hadron decay mode $qqH \rightarrow qq\tau\tau \rightarrow qq\ell\nu\nu j\nu$. In these analyses, $Z +$ jet production with $Z \rightarrow \tau\tau$ constitutes the principal background. The pattern of the analysis approximately follows the pattern set for WW decay. In order to detect the signal over background it is necessary to reconstruct the Higgs invariant mass. In both signal and background events, the H and Z bosons are emitted with significant p_T, and therefore the τs are produced with high boosts, causing the τ decay products to be approximately collinear in the laboratory reference frame. It is then possible to assume that the tau directions are given by the directions of the visible decay products, and thence the tau momenta and their invariant mass can be reconstructed. The invariant mass thus reconstructed is shown in Fig. 10. Given the presence of a peak, the background estimate could in principle be performed by subtraction of the side-bands. In practice, as seen in the figures, since the Higgs peak sits on the tail of the $Z \rightarrow \tau\tau$ mass distribution, a large uncertainty on the determination of the signal significance can come from the evaluation of the Z mass distribution. If an uncertainty of 10% on the background estimate is assumed, by combining all of the τ decay channels a significance above 5σ can be achieved between 115 and 140 GeV/c^2 for an integrated luminosity of 30 fb^{-1}. The measurement of this channel is very important, as it gives access of the coupling of the Higgs boson to the τ lepton.

4.3.3. The $qqH \rightarrow qq\gamma\gamma$ channel

Given that the two photon decay of the Higgs is favourable for detection at the LHC, but the since inclusive channel has a large irreducible background, it is of interest to check the vector boson fusion production of this channel, i.e. qqH, $H \rightarrow \gamma\gamma$. Two electromagnetic clusters are requested in the central detector together with a pair of jets with a separation of at least 4 units in η. The dominating backgrounds are $\gamma + 3$ jets and especially $\gamma\gamma + 2$ jet events. The resulting signal significance for 60 fb^{-1} of integrated luminosity amounts to slightly more than 3σ for a Higgs particle in the mass range of 115–130 GeV/c^2, reducing to a bit less than 2.5σ for higher masses, up to 150 GeV/c^2. Hence this channel is less sensitive than the inclusive $H \rightarrow \gamma\gamma$ analysis, but it can contribute to establish the discovery of the Higgs in the two-photon final state.

4.4. Exclusive Higgs production

Recently [18,19] the possibility to produce a Higgs particle in a rather clean environment at the LHC has been extensively discussed: the central exclusive production (CEP). The diagram to produce the Higgs is shown in
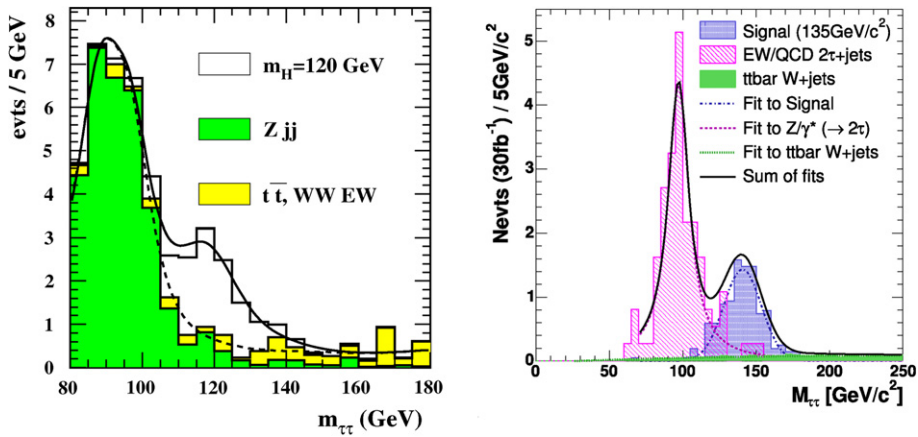
Fig. 10. (Left) The reconstructed $\tau\tau$ invariant mass for a Higgs boson signal of 120 GeV/c^2 in the $e\mu$ channel above all backgrounds after application of all cuts except the mass window cut around the Higgs boson mass (from Ref. [2]). (Right) The same, for the ℓ-had channel and for a Higgs boson with $m_H = 135$ GeV/c^2 (from Ref. [4]). The number of signal and background events are shown for an integrated luminosity of 30 fb^{-1} in both figures.
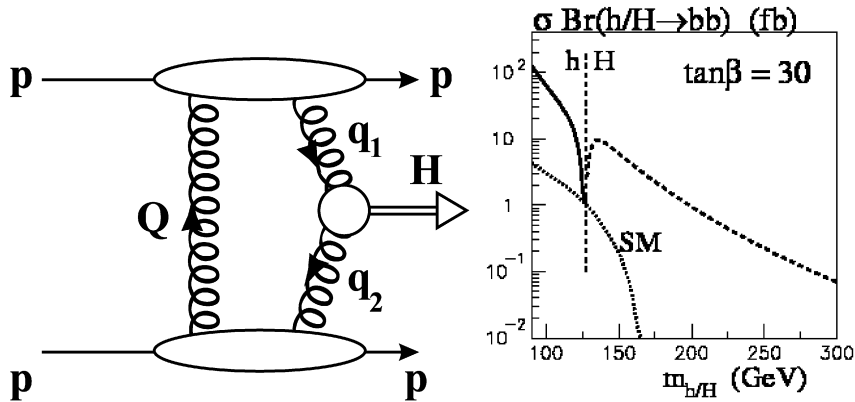

Fig. 11. (Left) Diagram for the CEP process; (Right) Cross-section for SM and MSSM exclusive Higgs production (from Ref. [22]).

Fig. 11(left): $pp \to pHp$. The protons remain intact and can be detected by near-beam detectors. Presently the LHC experiments are not equipped to detect these protons but the FP420 R&D Collaboration is completing a proposal to instrument the region at 420 m away from the interaction region [20]. With these detectors the protons of CEP Higgs production in the mass range of $70 < M_H < 150$ GeV/c^2 can be detected.

These protons allows to measure the mass of the centrally produced system with a precision of 1–2 GeV/c^2 via the missing mass to the incoming beam particles: $M^2 = (p_1 + p_2 - p_1' - p_2')^2$ with (p_1, p_2) and (p_1', p_2') the 4-vectors of the incoming and outgoing protons respectively. In fact, by detecting and tagging the process through the outgoing protons, it is possible in principle to analyse Higgs production regardless of the decay products, similar to HZ production at a linear e^+e^- collider. Moreover, the CEP requirement suppresses the QCD background processes such as exclusive $gg \to bb$ in leading order. This leads to the promise that the decay mode $H \to bb$ could be observed above background in CEP. Furthermore, to a very good approximation the central system is constrained to be a colour singlet, $J_Z = 0$ state, and, due to the strongly constraint three particle final state, the measurement of azimuthal correlations between the two scattered protons will allow to determine the CP quantum numbers of the produced central system [21].

The downside of this process is that the cross-section is relatively small as shown in Fig. 11(right): a few fb for the SM Higgs. The process can however be a factor 10 or more larger in the MSSM for relatively high $\tan\beta$ as shown in Fig. 11(right) and recently also discussed in [23,24]. Recent studies [25] show that the Standard Model Higgs measurement will be challenging in CEP for the $H \to bb$ mode. However, the decay mode $H \to WW^{(*)}$ is
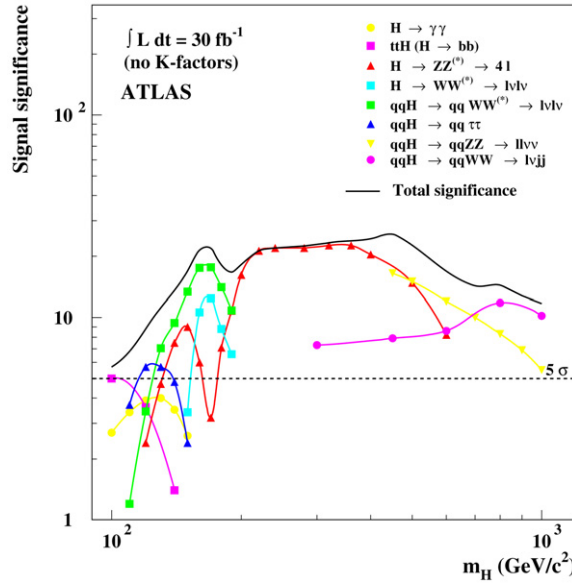
Fig. 12. ATLAS sensitivity for the discovery of a Standard Model Higgs boson for an integrated luminosity of 30 fb^{-1} over the full mass region. The signal significance is plotted for the individual channels. The black continuous line gives the combination of all channels. Systematic uncertainties on the background have been included for the vector boson fusion channels ($\pm 10\%$) and for the $H \to WW^{(*)} \to \ell\nu\ell\nu$ channel ($\pm 5\%$).
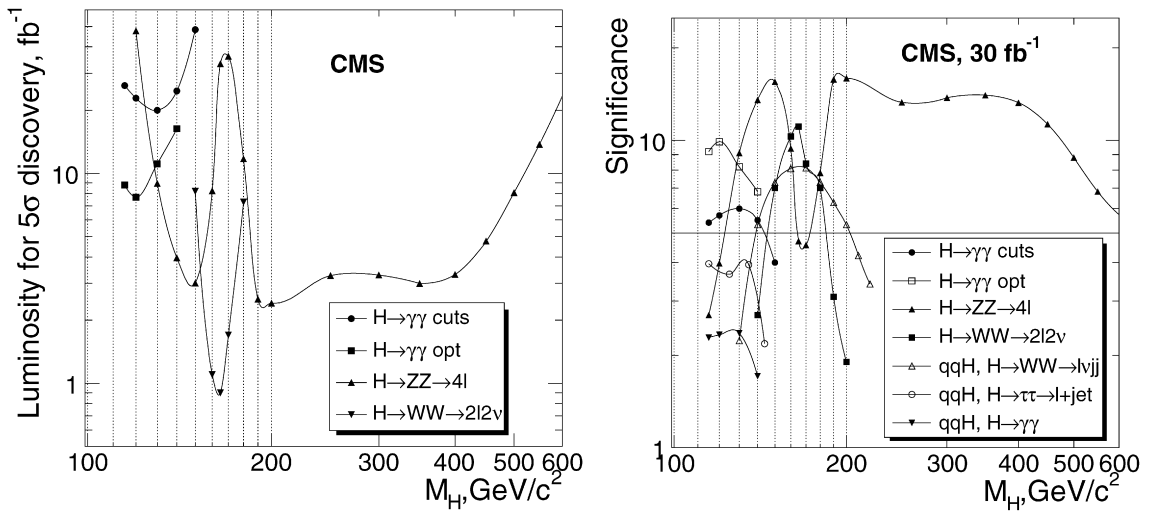

Fig. 13. (Left) The integrated luminosity needed for the 5σ discovery of the inclusive Higgs boson production $pp \to H + X$ with the Higgs boson decay modes $H \to \gamma\gamma$, $H \to ZZ \to 4l$, and $H \to WW \to 2l2\nu$. (Right) The signal significance as a function of the Higgs boson mass for 30 fb^{-1} of integrated luminosity for the different Higgs boson production and decay channels (from Ref. [4]).

measurable for masses up to about 140 GeV/c^2 [26]. About 10 events are expected for 30 fb^{-1} after trigger and detector cuts, with essentially no background.

4.5. Combined discovery potential

The combined ATLAS Higgs boson discovery potential over the full mass range, $100 < m_H < 1000$ GeV/c^2, assuming an integrated luminosity of 30 fb^{-1} is shown in Fig. 12. The full mass range up to ~ 1 TeV/c^2 can be covered with a signal significance of more than 5σ with several discovery channels available at the same time. In this evaluation no K-factors have been included. The combined CMS Higgs discovery potential for the principal decay
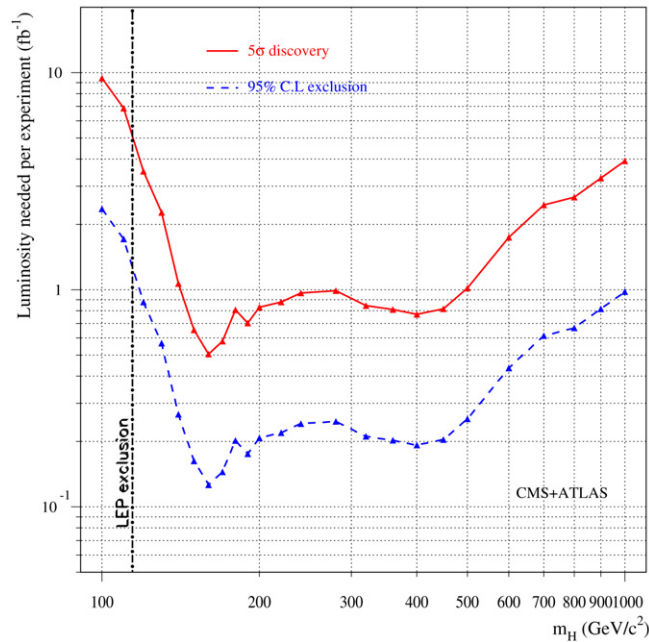
Fig. 14. The prospects for discovering or excluding at 95% CL a Standard Model Higgs boson in initial LHC running, as a function of its mass, combining the capabilities of ATLAS and CMS (from Ref. [27]).

channels is shown in Fig. 13. It shows the luminosity needed for a 5σ discovery as function of mass of the Higgs, and the significance that can be reached with 30 fb^{-1}. The conclusions are similar to those of ATLAS.

In all, a luminosity of about 10 fb^{-1} will allow us to cover almost the whole region for a discovery of the Higgs. Equally interesting is the luminosity needed to exclude Higgs masses. This is shown in Fig. 14 (from [27]) for 95% CL exclusion limits, for combined ATLAS and CMS data. Clearly the first 1 fb^{-1} will already be very revealing.

5. Measurement of Higgs parameters

If the SM Higgs exists, it should appear as an excess above the Standard Model expectation in one or more of the search channels described above. The next task for the experiments will be to measure the properties of the observed new particle. The measurement of the mass will fix the last unknown parameters in the Standard Model. The first step thereafter should be to verify whether the new particle is a scalar, and if its CP properties match those expected for the Higgs. Once the Higgs mass is fixed, under the minimal assumption that the structure of the Higgs sector comprises only one Higgs doublet, the width and the coupling are predicted with great precision by the Standard Model. In order to have the full verification of the SM Higgs, these parameters have to be measured. We will briefly review in the following the measurement potential for these parameters in ATLAS and CMS.

5.1. Mass and width

The most promising channels to measure the width and mass of the Higgs boson are $H \to \gamma\gamma$ and $H \to 4$ leptons. A recent estimate of the statistical precision that can be achieved with 30 fb^{-1} is shown in Fig. 15. This is not expected to be deteriorated much by systematical errors. It confirms that a precision of 0.1% to 1%, depending on the mass, is within reach, as reported earlier [1,28].

The width of a Standard Model Higgs can be determined directly only for masses larger than 200 GeV/c^2, where the intrinsic width of the resonance is larger than the experimental resolution. The channel $H \to ZZ \to 4$ leptons can be used, and the precision on the width is about 6% for the mass range of $300 < M_H < 700$ GeV/c^2 [1]. In the low mass region, the Higgs width can be constrained only indirectly by adding all observed decay modes, as proposed in [29], to a precision of 10–20%.
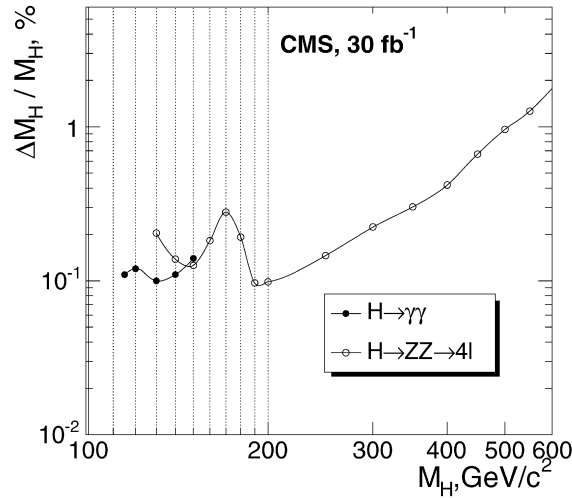
Fig. 15. The statistical precision of the Higgs boson mass measurement for 30 fb^{-1} using inclusive Higgs boson production $pp \to H + X$ and the $H \to \gamma\gamma$ and $H \to ZZ \to 4\ell$ decay modes (from Ref. [4]).
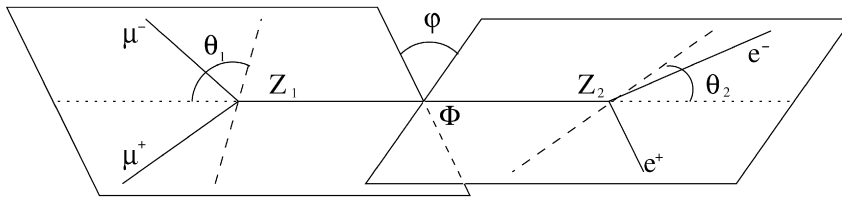

Fig. 16. Definitions of the angles in the $\Phi \to ZZ \to e^+e^-\mu^+\mu^-$ process.

5.2. Spin and CP

One of the important questions that will need to be answered is whether the found Higgs candidate has the right spin and CP properties. This will not be an easy task at the LHC. So far, candidate processes are the study of angular correlations in $H \to ZZ$ decays, the study of correlations in the VBF process, and the earlier mentioned central exclusive production channel. The fact that the decay rate $H \to \gamma\gamma$ will be observed rules out the $J = 1$ hypothesis.

In the study of the CP-parity of the Higgs boson decaying into 4 leptons, two angular distributions can be analysed see Fig. 16. The first one is a distribution of the angle φ (called plane or azimuthal angle) between the planes of two decaying Zs in the Higgs boson rest frame. The second one is a distribution of the polar angle θ, in the Z rest frame, between momentum of negatively charged lepton and the direction of motion of Z boson rest frame. Here we show results from a recent CMS study, as function of a parameter ξ that parametrises the CP state (see [4]), for scalar ($\xi = 0$), pseudoscalar ($\xi = \pi/2$) and CP-violating Higgs boson states, the latter for $\tan\xi = \pm 0.1,\ \pm 0.4, \pm 1$ and ± 4.

The influence was studied of the enhancement (or suppression) factor C^2 of the Higgs boson production cross-section times branching ratio, with respect to the Standard Model $C^2 = (\sigma \times Br)/(\sigma_{SM} \times Br_{SM})$ on the accuracy of the ξ measurement and thus, on possibility to exclude the Standard Model scalar Higgs boson. Fig. 17 shows the minimal value of the factor C^2 needed to exclude the SM Higgs boson at $N\sigma$ level ($N = 1, 3$), where $N = \xi/\Delta\xi$, as a function of the parameter ξ.

An ATLAS analysis used the same channel to study the same angles φ and θ as noted in Fig. 16. With 100 fb^{-1} the separation from the SM for Higgs masses above 250 GeV/c^2 is more than 8σ. At lower masses the discrimination is more difficult, especially below $M_H = 200$ GeV/c^2.

Recently, the W-boson fusion channel has been suggested as an analyzer of the ϕVV coupling. The method is applicable for Higgs masses less than 200 GeV/c^2 [30]. The angular correlations of the tag jets contain information on the structure of the $VV \to \phi$ tensor. A result of a fast simulation, using the $H \to \tau\tau$ and $H \to WW$ channel have been performed [31]. Fig. 18 shows distributions of $\Delta\phi_{\mathrm{jetjet}}$ for these two channels, for three different couplings:
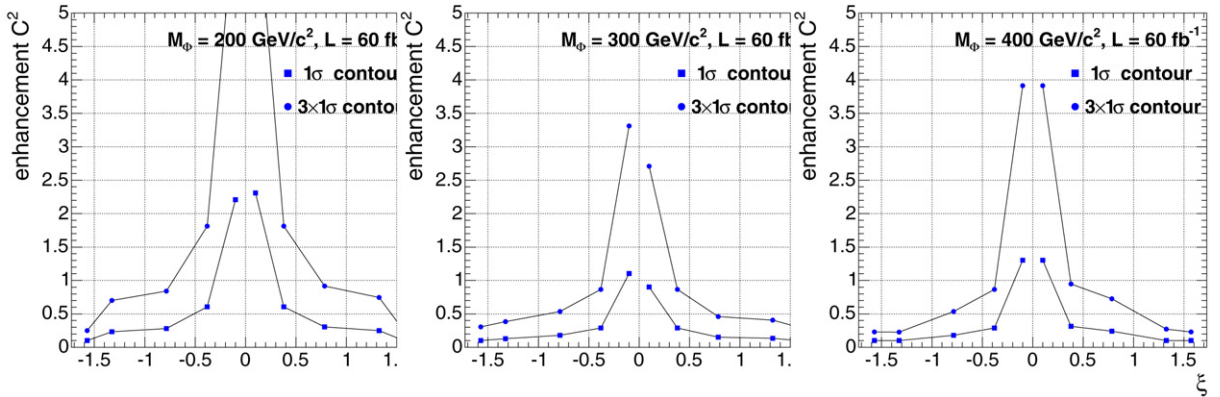
Fig. 17. The minimal value of the factor C^2 needed to exclude the Standard Model, scalar Higgs boson at $N\sigma$ level ($N = 1, 3$) as a function of the parameter ξ for the Higgs boson masses M_Φ=200, 300 and 400 GeV/c^2 (from left to right) at 60 fb^{-1} (from Ref. [4]).
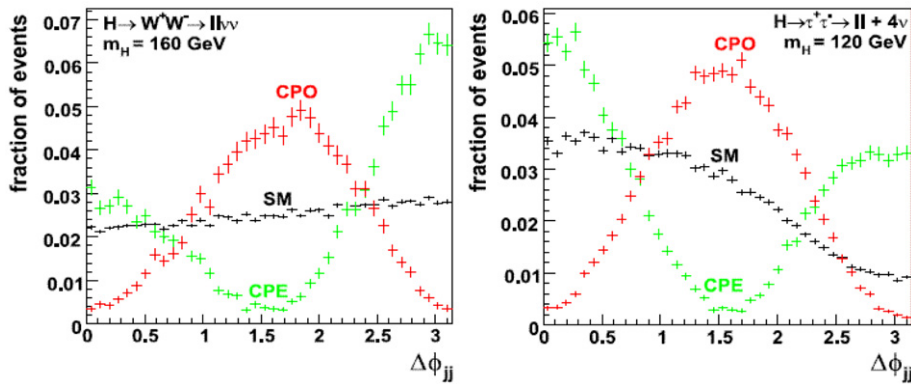

Fig. 18. Distribution of the variable $\Delta\phi_{jj}$ with high statistics for signal events. Distributions are shown for each of the three different couplings and two channels studied (from Ref. [31]).

Standard Model, a CP odd anomalous coupling and a CP even anomalous coupling. For a SM model Higgs boson it is found that purely anomalous couplings are expected to be excluded at a confidence level corresponding to 2σ or more at $m_H = 120$ GeV/c^2 and more than 5σ at $m_H = 160$ GeV/c^2 with 30 fb^{-1} of data.

5.3. Couplings

The large variety of production modes and decay channels which can be employed for the discovery of the Higgs boson opens the possibility to measure the couplings of the Higgs to the third generation fermions and to the gauge bosons. These couplings are predicted to be different from the Standard Model one, e.g. in models with two Higgs doublets, as discussed e.g. in [7], depending on the parameters of the sector. In particular, for $m_H < 2m_Z$, the Higgs width is small, and the rates $\sigma \cdot BR(H \to f\bar{f})$ are to a good approximation proportional to $\Gamma_i \cdot \Gamma_f / \Gamma$, where Γ_i and Γ_f are the Higgs boson partial widths involving the couplings at production and decay, respectively, and Γ is the total width of the Higgs boson.

A study has been performed on the extraction of the Higgs partial widths [32] based on the studies performed for the channels shown in Table 3. Assuming that the measured values will be the ones of the Standard Model, the couplings are evaluated through a likelihood function. The inputs are the expected number of events after analysis cuts for each channel for a given value of the integrated luminosity. Systematic errors both on signal and expected backgrounds are incorporated in the calculation, as well as systematic uncertainties on theory. The result of the fit are relative branching ratios which are identical to ratios of partial widths. The partial width for $H \to WW$ is used as normalisation, as it can be measured over the whole range with reasonable accuracy. The expected uncertainties on

Table 3
List of all studies used in the global likelihood fit performed in Ref. [32]; each channel has been used in the mass range indicated

Production mode	Decay mode	Mass range (GeV/c^2)
Gluon fusion	$H \to ZZ^{(*)} \to \ell\ell\ell\ell$	110–200
	$H \to WW^{(*)} \to \ell\nu\ell\nu$	110–200
	$H \to \gamma\gamma$	110–150
Vector boson fusion	$H \to ZZ^{(*)} \to \ell\ell\,\ell\ell$	110–200
	$H \to WW^{(*)} \to \ell\nu\,\ell\nu$	110–190
	$H \to \tau\tau \to \ell\nu\nu\ell\nu\nu$	110–150
	$H \to \tau\tau \to \ell\nu\nu had\nu$	110–150
	$H \to \gamma\gamma$	110–150
$t\bar{t}H$ production	$H \to WW^{(*)} \to \ell\nu\ell\nu(\ell\nu)$	120–200
	$H \to b\bar{b}$	110–140
	$H \to \gamma\gamma$	110–120
WH production	$H \to WW^{(*)} \to \ell\nu\ell\nu(\ell\nu)$	150–190
	$H \to \gamma\gamma$	110–120
ZH production	$H \to \gamma\gamma$	110–120

the ratios of partial widths are shown in the left panel of Fig. 19, for an assumed luminosity of 300 fb^{-1}. The ratio Γ_Z/Γ_Z can be measured with a 10–20% precision for $m_H > 130$ GeV/c^2, whereas the fermionic width Γ_b/Γ_Z and Γ_τ/Γ_Z are only measured with a precision of order 30% to 60%.

These measurements are done with essentially no theoretical assumption and only using the observable decays. One can make additional moderate assumptions, i.e. that only known SM particles couple to the Higgs, and that the coupling to light fermions is not too much enhanced. In this case both the production processes and the decays can be expressed in terms of the Higgs couplings g_W, g_Z, g_τ, g_b, g_t. In particular the Yukawa coupling g_t can be measured from the associated production g_t. The exact dependence of the observables from the coupling is calculated theoretically and input in the fit. The relative errors on the measurements of ratios of couplings are shown in the right panel of Fig. 19 for 300 fb^{-1} and one experiment. Thanks to its contribution to both gluon fusion and ttH the coupling to the top can be constrained at the 10–20% level. In a recent study [33] these measurements were discussed in the framework of a general two-doublet model. In general, if only Higgs singlets and doublets are present in the model, the constraint $g_{W/Z}^2 < g_{W/Z}^2(SM)$ can be used. If this constraint is applied, assuming an integrated luminosity of 300 fb^{-1} (100 fb^{-1} for vector boson fusion) typical accuracies of 20–30% for the absolute couplings can be achieved for $m_H < 160$ GeV/c^2. For masses above the W-pair threshold the measurement of the W and Z partial width can be performed with an accuracy at the level of $\pm 10\%$.

5.4. Higgs boson self coupling

The definitive test of the Higgs mechanism will be the demonstration that the Higgs potential has the form $V_H = \frac{m_H^2}{2}H^2 + \frac{m_H^2}{2v}H^3 + \frac{m_H^2}{8v^2}H^4$, where $v = (\sqrt{2}G_F)^{-1/2} = 246$ GeV/c^2 is the Higgs vacuum expectation value. The coefficients of the trilinear term $\lambda_{HHH} = \frac{m_H^2}{2v}$ and the one on the quadrilinear term $\lambda_{HHHH} = \frac{m_H^2}{8v^2}$ are given by the Standard Model. The phenomenological and experimental investigations have concentrated on the trilinear terms which gives rise to the production of two Higgs bosons.

The most favourable channel is the one where both Higgs bosons decay to WW, and two of the W decay leptonically, yielding a final state with two charged leptons, two neutrinos and four jets. This channels has been the subject of several studies [34–36]. A large background comes from $t\bar{t}$ and from multiple gauge boson production. In order to suppress these backgrounds final state with two same-sign leptons offers the best sensitivity. The conclusion of these studies is that with 300 fb^{-1}, the ultimate luminosity expected at the LHC a determination of the Higgs boson self-coupling will be very challenging. A measurement with reasonable errors will require a luminosity upgrade of the LHC.
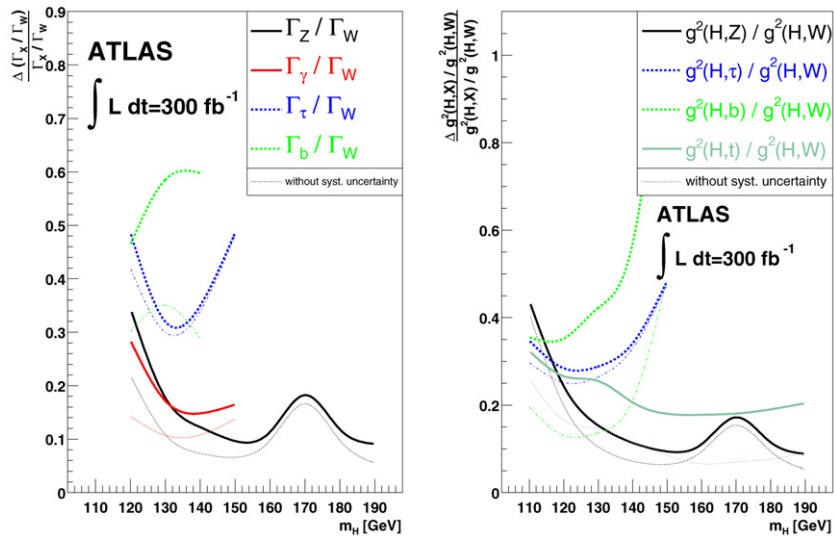
Fig. 19. The expected relative errors for the measurement of relative branching ratios (left) and relative couplings (right), normalised to those of the $H \to WW$ decay and assuming an integrated luminosity of 300 fb^{-1} for one experiment. The dashed lines give the expected relative error without systematic uncertainties (from Ref. [32]).

6. Conclusions

The LHC has a huge discovery potential for the Standard Model Higgs. The complete range of interest, up to a Higgs mass of 1 TeV/c^2 can be covered. A discovery of the Higgs particle can be expected in the most favourable case with perhaps already 1–2 fb^{-1}, for a Higgs boson with a mass close to 160 GeV/c^2. The most luminosity demanding regions are the one for a low Higgs mass (<130 GeV/c^2) and the one for the high Higgs mass (>500 GeV/c^2), but a total of about 10 fb^{-1} seems sufficient to cover the full mass range. Hence, according to present expectation, such data sample should be available for analysis by 2010. Reversely, already with less than 1 fb^{-1} the experiments will be able to exclude at the 95% level large regions in the possible Higgs mass space.

The most important channels for the Higgs discovery are still the $H \to \gamma\gamma$, $H \to ZZ^{(*)}$ and $H \to WW^{(*)}$ decays. At low Higgs masses vector boson fusion channels will play an important role as well, particularly for Higgs decay modes into τ particles. Associated production will help to establish the signal but in general the sensitivity is smaller than for the inclusive production channels. The Higgs decay in b-quarks remains one of the important challenges at the LHC, particularly after the re-analyses of the ttH channel which is unlikely to play a significant role in the first 30 fb^{-1} collected at the LHC. Possibly exclusive central production can add information to this decay channel.

With 100 fb^{-1} or more of data, Higgs properties will be studied in detail, such as the mass and width (directly or indirectly depending on the mass of the Higgs), and its CP properties.

In all, the start-up of the LHC is eagerly awaited for. In 2008 the first collisions will be collected, and the first Higgs hunting year is likely to be 2009. The experiments and analyses teams will be ready for this hunt, hence, if all goes as planned, the next 2–3 years will be very decisive for the "to be or not to be" of the Standard Model Higgs.

Acknowledgements

References

[1] ATLAS Collaboration, ATLAS detector and physics performance, Technical Design Report, CERN/LHCC 99-14/15 (1999), http://atlas.web. cern.ch/Atlas/GROUPS/PHYSICS/TDR/access.html.

[2] S. Asai, et al., Prospects for the search of a Standard Model Higgs boson in ATLAS using vector boson fusion, Eur. Phys. J. C 32 (2003) 209, ATLAS note SN-ATLAS-2003-024, hep-ph/0402254.

[3] CMS Collaboration: CMS physics: Technical Design Report v.1: Detector performance and software, CERN-LHCC-2006-001 (2006), http://cdsweb.cern.ch/search.py?recid=922757.

[4] CMS Collaboration, CMS physics: Technical Design Report v.2: Physics performance CERN-LHCC-2006-021 (2006) J. Phys. G: Nucl. Part. Phys. 34 (2007) 995, doi:10.1088/0954, http://cdsweb.cern.ch/search.py?recid=942733.

[5] S. Abdullin, et al., J. Phys. G 31 (2005) 71, hep-ph/0503067.

[6] V. Buscher, K. Jakobs, Int. J. Mod. Phys. A 20 (2005) 2523, hep-ph/0504099.

[7] J. Ellis, G. Ridolfi, F. Zwirner, C. R. Physique 8 (9) (2007) 999.

[8] A. Djouadi, hep-ph/0503172, 2005.

[9] U. Aglietti, et al., Tevatron-for-LHC Report: Higgs, FERMILAB-CONF-06-467-E-T, hep-ph/0612172, 2006.

[10] C. Anastasiou, K. Melnikov, F. Petriello, Nucl. Phys. B 724 (2005) 197, hep-ph/0501130.

[11] M. Spira, private communication.

[12] ATLAS Collaboration, ATLAS Technical proposal, CERN/LHCC/94-43 (1994), and Technical Design Reports of the detector subsystems, CERN/LHCC, http://atlas.web.cern.ch/Atlas/internal/tdr.html.

[13] CMS Collaboration, CMS Technical proposal, CERN/LHCC 94-38 (1994), and Technical Design Reports of the detector subsystems, CERN/LHCC, http://cmsinfo.cern.ch/Welcome.html/cmsdocsite.html.

[14] F. Ragusa, G. Rolandi, New J. Phys. 9 (2007) 336.

[15] M. Dittmar, H.K. Dreiner, Phys. Rev. D 55 (1997) 167, hep-ph/9608317.

[16] M.L. Mangano, M. Moretti, F. Piccinini, R. Pittau, A.D. Polosa, JHEP 0307 (2003) 001, hep-ph/0206293.

[17] J. Leveque, J.B. de Vivie, V. Kostioukhine, A. Rozanov, Search for the Standard Model Higgs boson in the $t\bar{t}H$, $H \to WW^{(*)}$ channel, ATLAS note, ATL-PHYS-2002-019.

[18] V. A Khoze, A.D. Martin, M.G. Ryskin, Eur. Phys. J. C 23 (2002) 311.

[19] A. De Roeck, V.A. Khoze, A.D. Martin, R. Orava, M.G. Ryskin, Eur. Phys. J. C 25 (2002) 391.

[20] M.G. Albrow, et al., FP420: An R & D proposal to investigate the feasibility of installing proton tagging detectors in the 420-m region at LHC, CERN-LHCC-2005-025, June 2005.

[21] V. A Khoze, A.D. Martin, M.G. Ryskin, Eur. Phys. J. C 34 (2004) 327, hep-ph/0401078.

[22] A. Kaidalov, V.A. Khoze, A.D. Martin, M.G. Ryskin, Eur. Phys. J. C 33 (2004) 261, hep-ph/0311023.

[23] S. Heinemeyer, et al., DCPT-07-80, IPPP-07-40, August 2007, arXiv: 0708.3052.

[24] B.E. Cox, F.K. Loebinger, A.D. Pilkington, MAN-HEP-2007-15, September 2007, arXiv: 0709.3035 [hep-ph].

[25] M. Albrow, et al. (CMS & TOTEM), Prospects for diffractive and forward physics at the LHC. CERN-LHCC-2006-039, CERN-LHCC-G-124, CERN-CMS-NOTE-2007-002, December 2006, 156 pp.

[26] B.E. Cox, Eur. Phys. J. C 45 (2006) 401, hep-ph/0505240.

[27] J.J. Blaising, et al., Potential LHC contributions to Europe's future strategy at the high-energy frontier, 2006.

[28] M. Hohlfeld, On the determination of Higgs parameters in the ATLAS experiment at the LHC, ATLAS internal note ATL-PHYS-2001-004, 2001.

[29] D. Zeppenfeld, R. Kinnunen, A. Nikitenko, E. Richter-Was, Phys. Rev. D 62 (2000) 013009, hep-ph/0002036.

[30] T. Figy, V. Hankele, G. Klamke, D. Zeppenfeld, Phys. Rev. D 74 (2006) 095001.

[31] C. Ruwiedel, N. Wermes, M. Schumacher, Eur. Phys. J. C 51 (2007) 385.

[32] M. Dührssen, Prospects for the measurement of Higgs boson coupling parameters in the mass range from 110–190 GeV/c^2, ATLAS note, ATL-PHYS-2003-030.

[33] M. Dührssen, et al., Phys. Rev. D 70 (2004) 113009, hep-ph/0406323.

[34] G. Azuelos, et al., J. Phys. G 28 (2002) 2453, hep-ph/0204087.

[35] U. Baur, T. Plehn, D. Rainwater, Phys. Rev. Lett. 89 (2002) 151801;
U. Baur, T. Plehn, D. Rainwater, Phys. Rev. D 68 (2003) 033003.

[36] F. Mazzucato, A. Blondel, A. Clark, Studies on the measurement of the SM Higgs self-couplings, ATLAS note, ATL-PHYS-2002-029.